PAPER

A bio-inspired electrocommunication system for small underwater robots

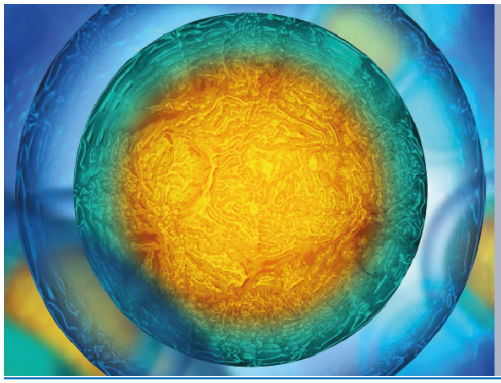

Bioinspiration & Biomimetics

PAPER

RECEIVED
3 January 2017

ACCEPTED FOR PUBLICATION
21 February 2017

PUBLISHED
29 March 2017

A bio-inspired electrocommunication system for small underwater robots

Wei Wang[1], **Jindong Liu**[2], **Guangming Xie**[1], **Li Wen**[3] **and Jianwei Zhang**[4]

[1] State Key Laboratory of Turbulence and Complex Systems, and Intelligent Control Laboratory, College of Engineering, Peking University, Beijing 100871, People's Republic of China
[2] Hamlyn Centre, Imperial College London, London, SW7 2AZ, United Kingdom
[3] School of Mechanical Engineering and Automation, Beihang Univerisity, Beijing 100191, People's Republic of China
[4] TAMS Group, Department of Informatics, University of Hamburg, 22527 Hamburg, Germany

E-mail: xiegming@pku.edu.cn

Keywords: electrocommunication, underwater communication, bio-inspired communication, underwater robots, robotic fish

Supplementary material for this article is available online

Abstract

Weakly electric fishes (Gymnotid and Mormyrid) use an electric field to communicate efficiently (termed electrocommunication) in the turbid waters of confined spaces where other communication modalities fail. Inspired by this biological phenomenon, we design an artificial electrocommunication system for small underwater robots and explore the capabilities of such an underwater robotic communication system. An analytical model for electrocommunication is derived to predict the effect of the key parameters such as electrode distance and emitter current of the system on the communication performance. According to this model, a low-dissipation, and small-sized electrocommunication system is proposed and integrated into a small robotic fish. We characterize the communication performance of the robot in still water, flowing water, water with obstacles and natural water conditions. The results show that underwater robots are able to communicate electrically at a speed of around 1 k baud within about 3 m with a low power consumption (less than 1 W). In addition, we demonstrate that two leader-follower robots successfully achieve motion synchronization through electrocommunication in the three-dimensional underwater space, indicating that this bio-inspired electrocommunication system is a promising setup for the interaction of small underwater robots.

1. Introduction

With the increasing requirements of high maneuverability, long duration, energy saving and even stealth for autonomous underwater vehicles (AUVs), researchers have been turning to a great variety of sources for inspiration [1, 2]. Many kinds of bio-inspired underwater robots, such as fish robot [3–6], snake robot [7, 8], salamander robot [1], dolphin robot [9] and turtle robot [10], have been developed by learning from aquatic animals in nature. These studies have mainly focused on dynamic modeling [11], locomotion control [1, 9, 12, 13], swimming efficiency [14], and perception [15], and have progressively advanced the development of underwater robotics.

Recently, there has been a growing interest in using large numbers of small underwater robots to study cooperative control [16–18]. Such swarms offer potentials to increase sensor density within the same or cost-effective system and provide excellent adaptability and flexibility in task execution, such as patrolling seaports, searching and rescuing. Bio-inspired underwater swarm robots can also serve as a controllable high-fidelity platform to study collective behaviors [19]. These swarm robots need to communicate underwater for information relay, motion coordination and formation control. However, as one of the essential capacities of robots, communication is particularly challenging for bio-inspired/small underwater robots that typically work in limited water environment and have stringent power and size constraints. The well established electromagnetic communication methods (e.g. 3G/4G, WiFi, Bluetooth) that are commonly used in the air, can barely work underwater. While acoustic communication has problems of large doppler shifts and multi-path

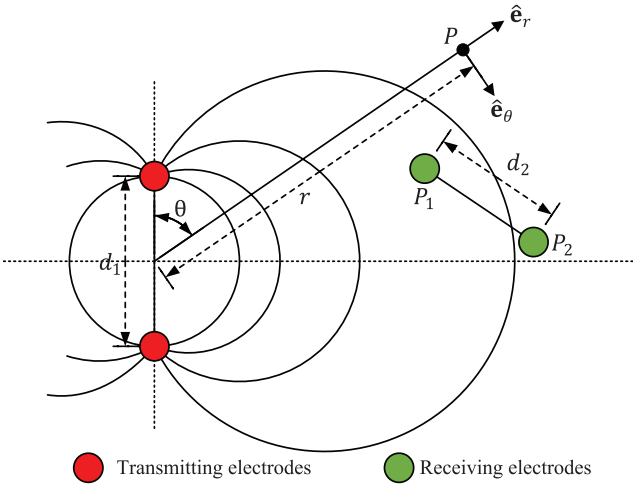

Figure 1. Schematic diagram of simplified electrocommunication model. P is one point near the transmitting electrodes; $\hat{\mathbf{e}}_r$ and $\hat{\mathbf{e}}_\theta$ are unit vectors in the radial and azimuthal directions in polar coordinates; d_1 is the distance between the transmitting electrodes and d_2 is the distance between the receiving electrodes; r is the distance between point P and the midpoint of transmitting electrodes and θ is the polar angle of point P.

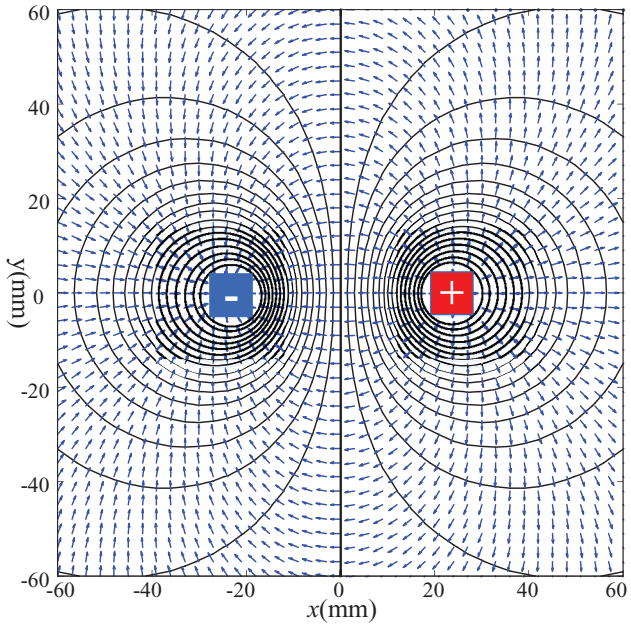

Figure 2. A planar electric field generated by a pair of electrodes fixed at +2 V and −2 V with a distance of 52 mm.

effects when robots are engaged in highly confined aquatic environments (e.g. shallow waters, narrow pipes, tunnels and caves [20]). In addition, current acoustic instruments are typically bulky and high-power, unaffordable to small underwater robots [21]. Hotspot optical communication cannot work in unclear water due to the requirement for a line of sight while communicating [22, 23]. Therefore, an alternative communication modality would be significant and is in urgent need of being developed for small underwater robots, especially in conditions where neither acoustic nor optical communication work. An example can be found in Morgansen's group [24, 25], where a specific radio frequency (RF) transceiver was designed to enable short-range underwater communication of small underwater vehicles.

Nature has already invented an exotic sense, the electric sense, which is used for localization and communication by several hundreds of fish species of the *Gymnotid* and *Mormyrid* families (collectively known as weakly electric fishes) [26, 27]. As an adaptation to their environment, weakly electric fishes have developed the ability to produce and perceive electric signals, similar to active sensing systems like radar and sonar. In particular, electric fishes communicate electrically (termed electrocommunication) by one fish generating an electric field and a second individual receiving that electric field with its electroreceptors and decoding the information with its nervous system [28]. Electric signals are generated by a specific organ called electric organ discharge (EOD) in weakly electric fishes. Signal frequencies, waveforms and time delay can be identified in electrocommunication. These fishes can

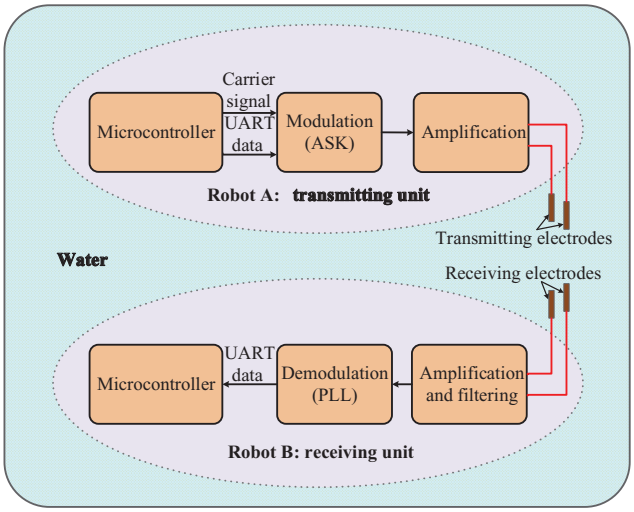

Figure 3. Overall design of electrocommunication system.

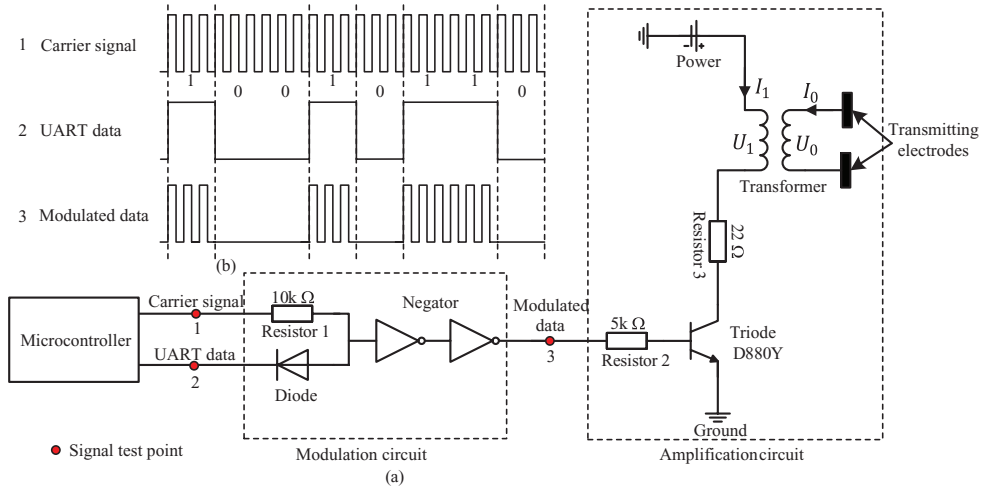

Figure 4. The transmitting unit of the artificial electrocommunication system. (a) The schematic diagram of the transmitting circuit; (b) the corresponding signal waveform in the three signal test points.

communicate electrically with each other within five to ten body lengths [28]. Although electric fishes are limited to a short communication range, the electric signals remain uncorrupted by echo and reverberation compared with sound and light. As a result, temporal features of electric signals remain constant during transmission and stable underwater communication is therefore possible.

Inspired by electric sensing, several artificial electrolocation systems have been developed for underwater target localization [29] and control of underwater robot groups [30]. The principle of electrolocation is that nearby objects with different impedance from water will distort the self-generated electric field of an underwater robot, and that an array of electrode sensors on that robot can detect the distortions. Different from electrolocation, this paper designs an artificial electrocommunication system available for small underwater robots. Underwater communication with a similar working principle has been preliminarily explored in the literature [31–39]. However, these studies typically employed bulky commercial instruments to simply prove the communication feasibility or conduct channel characterization in a static environment. For example, both Esemann *et al* [38] and Friedman *et al* [37] adopted ready-made Universal Software Radio Peripherals, GNU Radio software and two computers to set up their communication links. Zoksimovski *et al* [39] utilized commercial acquisition card and pre-amplifier model to build their communication system and the received signals were post-processed in Matlab. In this paper, we aim at: (1) exploring the potentialities and the difficulties of developing a small-sized and low-dissipation electrocommunication system for small underwater robots, (2) integrating the communication system into an underwater robot and systematically characterizing the overall performance of the robotic communication system in conditions of still water, flowing water, water with obstacles and natural water, and (3) demonstrating that underwater robots can successfully achieve motion synchronization in a three-dimensional water

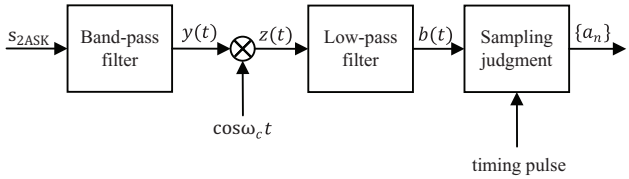

Figure 5. The coherent detection process for 2ASK signal demodulation.

space through electrocommunication. To our knowledge, this is the first time that electrocommunication is introduced into a small underwater bio-robotics, which would provide a promising approach for the cooperative control of future underwater robots.

This paper extends a previous conference paper [40] that initially designs an electric field communication system for remote control of an underwater robot. In this paper, we modify electronics to improve communication quality and carry out systematic experiments to characterize properties of electrocommunication in different water conditions. The first results here point out that robots can communicate successfully within about 3 m at a speed of around 1 k baud in an almost omnidirectional vision. Moreover, two leader-follower robots achieve autonomous motion synchronization through electrocommunication without extra coordination control. Furthermore, electrocommunication is a very inexpensive approach for underwater robots because the sensors are simply exposed conductors and the signal processing circuits are uncomplicated. Therefore, strengths like small size, low cost, low power, approximate omni-directivity, and high adaptability to water conditions, probably bring electrocommunication to be a useful complement to the usual suite of sensors provisioned on standard underwater robots in the near future.

The remainder of this paper is organized as follows. Section 2 derives a simple model to explain the principle of electrocommunication. A small-sized and low-power electrocommunication system is proposed for small underwater robots in section 3. The integration of electrocommunication and a small robotic fish prototype is described in section 4. Related experimental results in four water conditions and the discussion are provided in section 5. Section 6 concludes this paper with an outline of future work.

2. Principle of electrocommunication

In this section, we derive an analytical model for electrocommunication and analyse how key parameters such as electrode distance and emitter current affect the communication. Naturally, the mechanism of electrocommunication is complicated in electric fish. The fish intending to send signals generates an electric field by large arrays of electric cells on the body while the fish receiving signals senses the electric field and decodes electric signals by thousands of electroreceptors distributed all over the skin [41]. With the goal of developing an available electrocommunication system for underwater robots, it is reasonable and convenient to simplify the physical model of biological system as a pair of transmitting electrodes and a pair of receiving electrodes, as shown in figure 1. Such a simplified system features the basic principle of a biological communication system.

As illustrated in figure 1, a pair of transmitting electrodes generates an electric dipole field and a pair of receiving electrodes perceives the potential difference in the electric field. Since the electric signals change all the time in electrocommunication, the electric field generated by electric fish is electromagnetic wave essentially. Generally, both the conduction and displacement currents should be considered when the electric field changes over time. If however the time variation is sufficiently small, the displacement current is negligible and the conduction current is dominant. In this situation, it can be named as electric field communication.

In particular, for an alternating electric field $E(t) = E_0 \cos \omega t$ with the angular frequency ω in the water, the density of displacement current is defined as follow:

$$J_d = \frac{\partial D}{\partial t} \tag{1}$$

where $D = \varepsilon E$ is the electric displacement vector where ε is the permittivity of water. Then, the density of displacement current takes the form

$$J_d = -\omega \varepsilon E_0 \sin \omega t \tag{2}$$

Similarly, the density of conduction current J_c takes the form

$$J_c = \varepsilon E = \varepsilon E_0 \cos \omega t \tag{3}$$

Thus, the amplitude ratio of displacement current and conduction current is expressed as follows:

$$\frac{|J_d|}{|J_c|} = \frac{\varepsilon}{\sigma}\omega \tag{4}$$

where σ is the electric conductivity of water. The displacement current can be neglected if the following inequality exists:

$$\frac{|J_d|}{|J_c|} \ll 1 \tag{5}$$

For water, ε approximates $80\varepsilon_0$ at 20 degree Celsius where ε_0 is the free space permittivity and equals

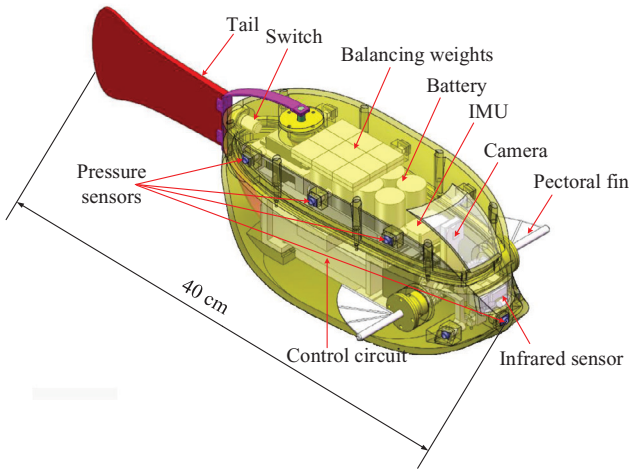

Figure 6. Mechanical and electrical configurations of the robotic fish.

Table 1. Technical specifications of the robot prototype.

Items	Characteristics
Dimension(L × W × H)	∼400 mm × 140 mm × 142 mm
Total mass	∼3.1 kg
Drive mode	DC servomotor (12.9 kg · cm)
Onboard sensors	Camera, IMU, pressure sensor, etc.
Maximum forward speed	∼1.0 BL s^{-1}
Power supply	9.6 V, 4.5 Ah battery
Operation time	∼5 h

8.85×10^{-12} F m^{-1}. Typically, σ is approximately 4 S m^{-1} for seawater while σ equals $0.01 \sim 0.1$ S m^{-1} for freshwater. In engineering, it is generally accepted that equation (5) holds if $|J_d|/|J_c| < 0.1$. According to this principle, the displacement current can be neglected for up to around 89 MHz in seawater and for up to several hundred kHz in freshwater (such as tap water and river water). The frequency of bioelectrical signals of electric fish is several kHz at most [42]. Thereby, electric fish electrocommunication is a kind of electric field communication.

It is still too complicated to analyse the performance of an alternating electric dipole conveniently. We need to further simplify the analysis by confining the system working in the near-field area [31]. The near-field assumption holds if the radius of the working area R satisfies the following inequation

$$R \ll \frac{\lambda}{2\pi} \tag{6}$$

where $\lambda = 2\pi\sqrt{\frac{2}{\omega\mu\sigma}}$ is the wave length and μ is the permeability of the water ($\mu = 1.257 \times 10^{-6}$ H m^{-1}). An alternating electric dipole working in the near-field area can be regarded as a quasi-static electric field and the electric field strength is described mathematically as follows [31],

$$\mathbf{E}(r,\theta) = \frac{I_0 d_1}{4\pi\sigma r^3}(2\cos\theta\hat{\mathbf{e}}_r + \sin\theta\hat{\mathbf{e}}_\theta) \tag{7}$$

where I_0 is the applied current between the pair of transmitting electrodes. Other parameters in equation (7) can be found in figure 1. To illustrate the electric field of equation (7) more clearly, we draw a planar electric field of two small electrodes fixed at +2 V and −2 V with an electric conductivity σ_m, as shown in figure 2. The right square in red (positive pole) is at +2 V and the left square in blue (negative pole) is at −2 V. Isopotential contours are placed at 100 mV increments and the bold line represents the 0 V contour.

Next, if a pair of receiving electrodes at a distance d_2 is near the electric field as shown in figure 1, the potential difference between P_1 and P_2 can be calculated as follows,

$$V = V_2 - V_1 = -\int_{P_1}^{P_2} \mathbf{E}(r,\theta) \cdot \mathrm{dl} \tag{8}$$

In particular, when the pair of receiving electrodes $\overline{P_1P_2}$ is parallel to the transmitting electrodes and on the axis of the dipole field (that is, $\theta = \pi/2$), the strength of the field will be $E = E_\theta = \frac{I_0 d_1}{4\pi\sigma r^3}$ and the potential difference between $\overline{P_1P_2}$ at d_2 can be written as follows,

$$V = \int_0^{d_2} E\mathrm{d}s = \frac{I_0 d_1 d_2}{4\pi\sigma r^3} \tag{9}$$

Generally speaking, for a receiver with a specific signal-to-noise ratio (SNR), the bigger potential difference the receiver can sense, the better communication quality the system will have and vice versa. From equations (7)–(9), we know that I_0, d_1, d_2, σ and r all contribute to the potential difference. For a specific water environment, the electric conductivity σ is assumed to be constant. Moreover, the distance r between the robots always change in practical application. As a consequence, for a specific artificial electrocommunication system, the emitter current I_0, the distance between transmitting electrodes d_1, and the distance between receiving electrodes d_2 can be enlarged as much as possible to improve the communication quality.

Furthermore, from equations (7) and (8), both the electric field strength and the potential difference decrease with distance in a general trend. Hence, we

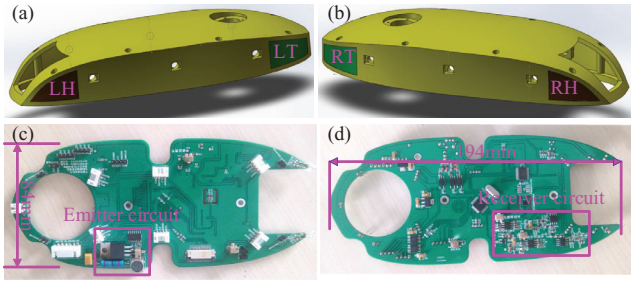

Figure 7. Electrode distribution and the communication circuit. LH, RH, LT and RT indicate the electrodes in different positions, where LH/RH for the left/right side of the head, and LT/RT for the left/right side of the tail. (a) Electrodes on the left side; (b) electrodes on the right side; (c) emitter circuit; and (d) receiver circuit.

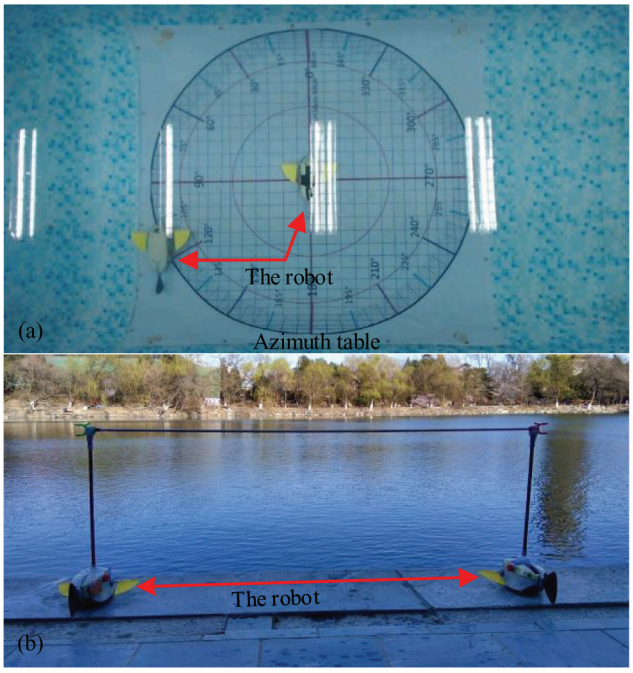

Figure 8. Experimental environments of electrocommunication. (a) Indoor swimming tank, and (b) Weiming Lake of Peking University.

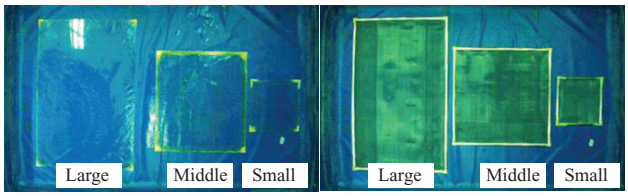

(a) (b)

Figure 9. Obstacles used in the experiments. (a) Three sizes of insulated obstacles; (b) three sizes of conductive obstacles.

can speculate that the communication performance declines with distance. On the other hand, the receiver will acquire different potential difference when the polar angle θ varies at one position. Therefore, we can also presume that the communication quality may change even when the receiver is at the same position. In extreme cases, when the receiver is perpendicular to the electric field, the potential difference of receiver will be zero, and the communication must be failed. To sum up, electrocommunication performance will shift with both spatial and angular distributions. Characterizing the performance of this novel electrocommunication will not only verify the simplified model but also be beneficial to robotic applications.

3. Artificial electrocommunication design

As mentioned earlier, an alternating electric dipole can be simplified as a quasi-static electric field by confining the system working in the near-field area. In this way,

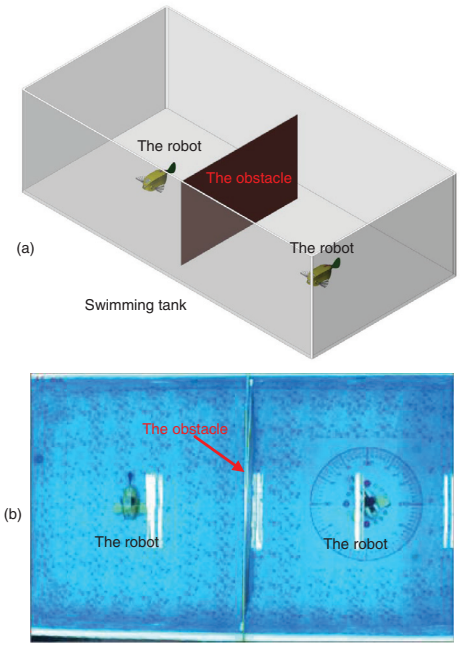

Figure 10. Illustration of the experiments with the largest size of obstacle. (a) Schematic scene; (b) experimental snapshot.

the communication performance can be characterized and analysed conveniently. Assuming the maximum communication range R of the system is 10 m, we can calculate the available signal frequency according to equation (6). Through calculation, we choose 40 kHz as the signal frequency of our electrocommunication system to basically satisfy the near-field assumption.

Developing a novel artificial electrocommunication system is difficult due to the unexplored scheme and implementation. For example, what kind of mode (current or voltage) should the electric field be emitted and measured by? What kind of form (analog or digital) should the signal be transferred by? Further, it is more challenging to design such an electrocommunication system for small underwater robots, which usually have size constraint, stringent power, limited hardware and conventional mobility in robotics. This section addresses these issues in the design of electrocommunication system.

3.1. Overall concept design

First, we choose to emit and measure the electric field in the form of voltage because voltage measurement is a common solution to traditional communication system. Second, we choose a digital method for communication since it is capable of higher bit rate delivery, higher anti-interference and easier integration with the robot microcontroller compared with analog method. Third, we use Universal Asynchronous Receiver/Transmitter (UART) protocol to transfer information, providing a convenient way to tune communication parameters (e.g. baudrate, data length and check bit) in practice. Moreover, UART also simplifies the demodulation circuit in system design.

Finally, the system scheme is formed and shown in figure 3.

It contains a transmitting unit, a receiving unit and two pairs of electrodes.

To acquire a better performance, the emitter should impose an electric field as strong as possible while the receiver should be able to sense the electric signal as weak as possible. However, if a system can impose an extremely strong electric field as well as pick up very weak electric signal, its circuit complexity and power consumption will be unaffordable to small underwater robots. Considering the limitations like small size, stringent power and low computational capability of small underwater robots, the communication system is particularly designed to be low power, small size and low complexity.

3.2. Transmitting unit design

According to the overall design of transmitting unit (as shown in figure 3) as well as the special limitations of small robots, an available solution is proposed and illustrated in figure 4(a). The transmitted signal is modulated to improve the communication performance. There are three basic modulation methods, amplitude shift keying (ASK), frequency shift keying (FSK) and phase shift keying (PSK). For simplicity, we employ ASK method to reduce the circuit complexity and power consumption. As previously mentioned, the frequency of the carrier signal is 40 kHz. Through many times explorations and trials, we determined a simple as well as efficient modulation circuit, as shown in figure 4(a). The circuit only consists of a resistor, a diode and two negators. The resistor and the diode modulate the signal jointly. Two negators are used to shape the modulated signal.

From the analysis in section 2, emitter current directly affects the communication performance. Hence, the modulated signals should be amplified before they are imposed into water. As shown in figure 4(a), the amplification circuit is also simple and efficient. It contains two resistors, one triode and one transformer. The amplification factor of the triode is set to be about 125, and Resistor 2 can be used to regulate the emitter current. The transformer is introduced to match the impedance of the circuit. The signal amplitude can be adjusted by altering the turns ratio of the transformer, changing the emitter current accordingly. In the experiments of this paper, the value of Resistor 2 is 5 KΩ and thus the current through the Resistor 3 is $I_1 = 125$ mA. It is easy to measure that $U_1 = 6.5$ V and $U_0 = 30$ V during communication. According to the following relationship in the transformer, $U_1/U_0 = I_0/I_1$, the emitter current can be acquired that $I_0 = 27$ mA. Then, the emitter power consumption P_t is calculated as $P_t = U_1 I_1 = U_0 I_0 = 0.81$ W. Such a low power would be affordable to the majority of miniature underwater robots. Considering that the communication radius can reach several meters under such a low circuit complexity and power condition, the

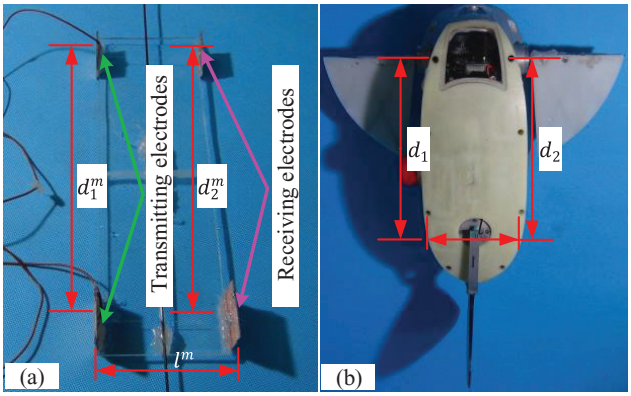

Figure 11. The fish model (a) and robotic fish (b) used in experiments. The fish model has identical layout with the robot where $d_1 = d_1^m, d_2 = d_2^m$ and $l = l^m$.

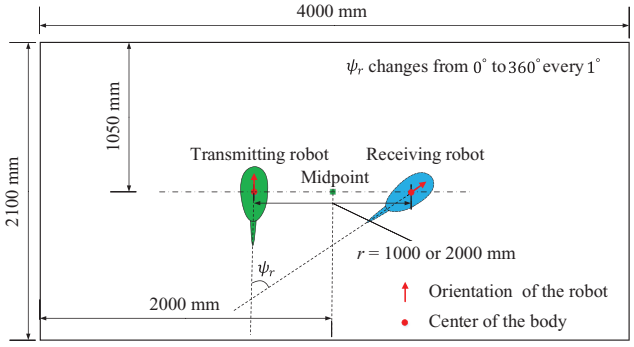

Figure 12. Experiment scene when the relative angle between the robots varies.

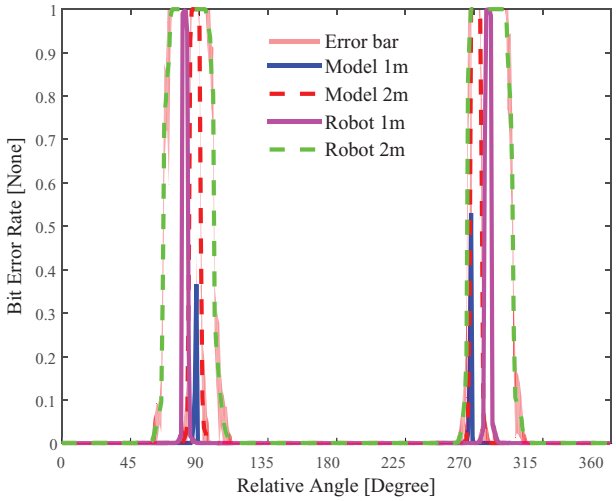

Figure 13. BER distribution for electrocommunication when the receiver adjusts its orientation at a distance of 1 m or 2 m in still water.

proposed emitter system for electrocommunication works efficiently.

3.3. Receiving unit design

Considering the size and power limitations of small robots, we should balance the sensitivity of the receiver with the circuit complexity in the receiving unit design.

Envelope detection and coherent detection are two common methods for ASK signal demodulation. We adopt coherent detection method to demodulate the received signal due to the fact that UART can take charge of some tasks during coherent detection, thereby reducing the circuit complexity and enhancing the system efficiency. Figure 5 draws the coherent detection process for ASK signal demodulation, where s_{2ASK} stands for the

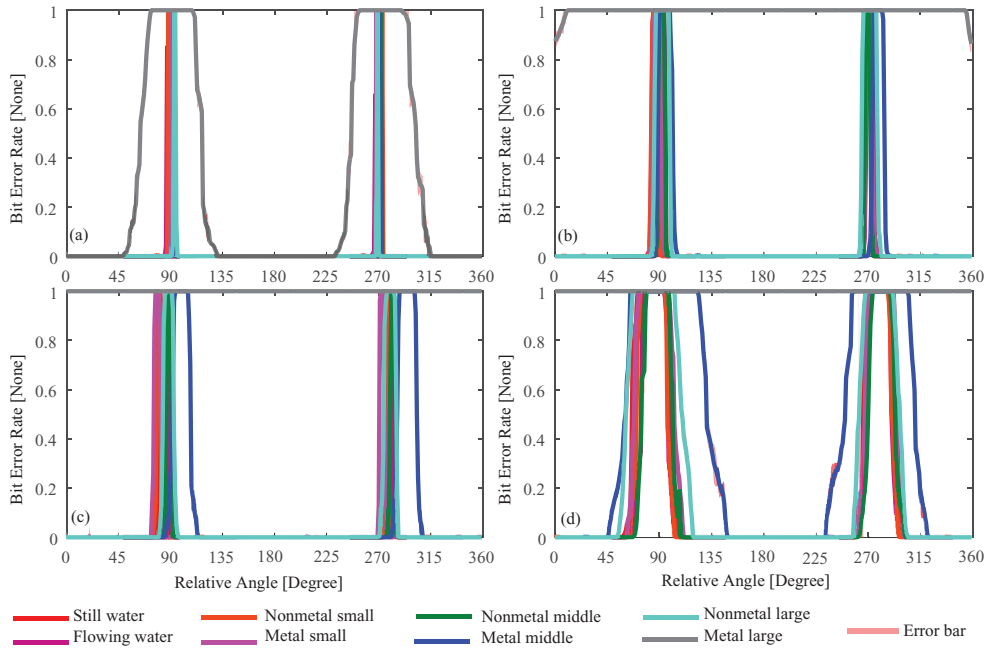

Figure 14. BER distribution for electrocommunication when the receiver adjusts its orientation at a distance of 1 m or 2 m in flowing water and water with obstacle. (a) Fish model with a distance of 1 m; (b) fish model with a distance of 2 m; (c) robot with a distance of 1 m; and (d) robot with a distance of 2 m.

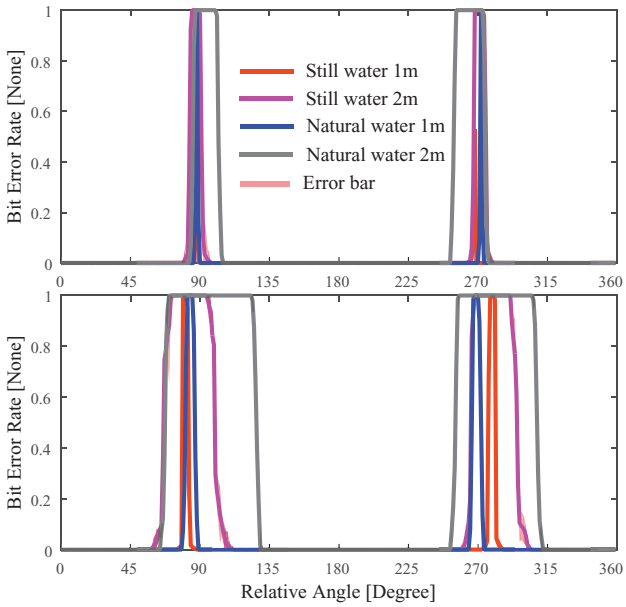

Figure 15. BER distribution for (a) the fish model and (b) the robot when the receiver adjusts direction at a distance of 1 m or 2 m in natural water.

signals picked up by the onboard receiving electrodes, and $y(t)$ stands for the filtered and amplified signals. A band-pass filter in the range 35 kHz $\sim$ 45 kHz was designed by using integrated operational amplifiers. After filtering, $y(t)$ can be expressed as follows

$$y(t) = b(t)\cos(\omega_c t) \tag{10}$$

where $b(t)$ stands for baseband signal, $cos(\omega_c t)$ stands for carrier signal and ω_c stands for angular frequency of carrier. To extract the baseband signal from $y(t)$, a local carrier signal $cos(\omega_c t)$ is generated to multiply $y(t)$. Then, the output $z(t)$ takes the form

$$z(t) = y(t)\cos(\omega_c t) = \frac{1}{2}b(t) + \frac{1}{2}(1 + \cos 2\omega_c t) \tag{11}$$

After that, a low-pass filter is employed to remove the high-frequency component in $z(t)$. Thus, the useful signal $b(t)$ is initially extracted. On account that $b(t)$ has distorted to a certain extent after low-pass filtering, a sampling judgment circuit is used to shape $b(t)$. In the end, the discrete baseband signal a_n is obtained.

Specifically, we use a tiny integrated phase-locked loop (PLL) chip to generate a local carrier signal

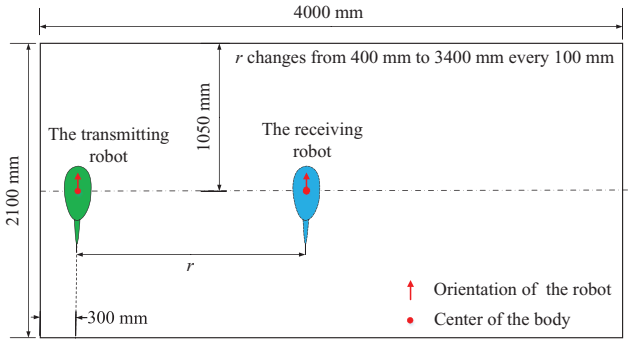

Figure 16. Experiment scene when the distance between the robots changes.

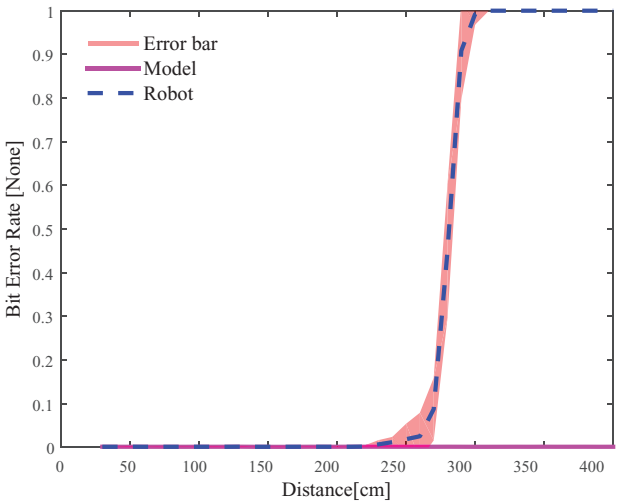

Figure 17. Electrocommunication BER varies with distance in still water.

$cos(\omega_c t)$. After that, $z(t)$ is directly imported into microcontroller's UART module. As mentioned earlier, UART takes over tasks like low-pass filtering, sampling judgment and timing pulse generation during coherent detection. In this way, the circuit size and complexity, and power consumption are further decreased. More importantly, the simplified circuits of receiver is more reliable because of the specialized UART circuit on the microcontroller.

4. Robotic electrocommunication system design

To demonstrate and characterize this electrocommunication system on small mobile robots, we integrate the system into our small robotic fish. This section describes the robot prototype and the integration of the electrocommunication system and the robot.

4.1. The robotic fish prototype

The robot body is inspired by a species of yellow-spotted ostraciiform boxfish living in coral reefs. As depicted in figure 6, the robot consists of a well-streamlined main body, a pair of pectoral fins and one caudal fin. The rigid shell involves upper and lower portions and offers a sufficient space for housing control circuits, sensors, actuators and rechargeable batteries. The upper portion is made of acrylonitrile butadiene styrene (ABS) plastic, while the lower portion adopts 6061 aluminium alloy to guarantee the firmness of propulsive units. The main controller of robot adopts a credit-card sized micro computer, Raspberry Pi. Meanwhile, three 32 bit auxiliary processors (STM32F103) are used for locomotion control, attitude calculation, and multiple sensor data acquisition and preprocessing, respectively. The technical specifications of the robot are listed in table 1. The robot is controlled by an artificial central pattern generator (CPG) network [43, 44]. Using the CPG controller, the robot is capable of multiple swimming behaviors, such as forward/backward swimming, turning, upward/downward swimming and rolling.

4.2. Integrating electrocommunication into robot

The model in section 2 indicates that the parameters I_0, d_1, d_2, σ and r all affect the communication performance. In the experiment, the electric conductivity of water σ is assumed to be constant and the imposed current I_0 is fixed. Moreover, the distance r between the robots always changes in experiments. As a consequence, d_1 and d_2 can be designed to

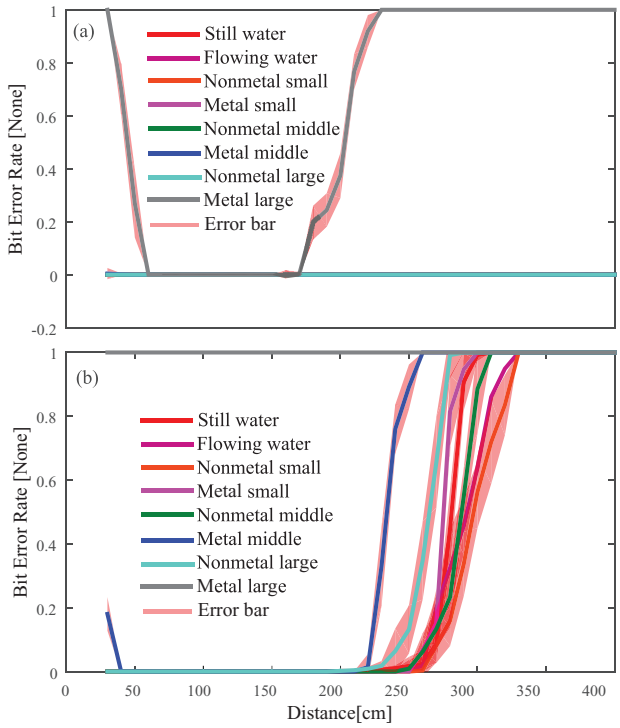

Figure 18. Electrocommunication BER varies with distance in flowing water and water with obstacles. (a) Fish model; and (b) the robot.

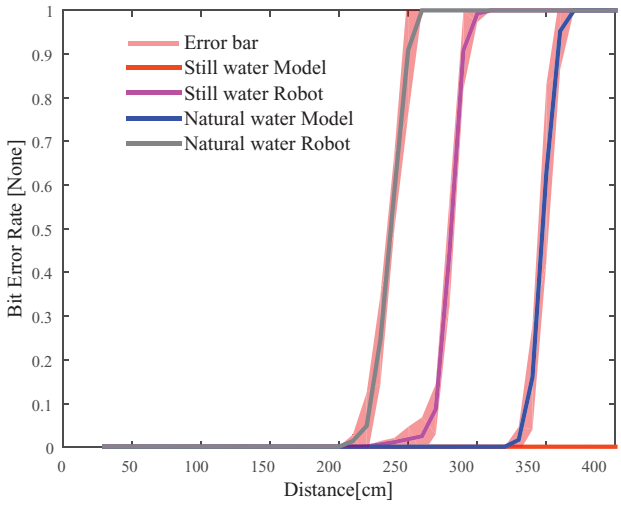

Figure 19. Electrocommunication BER varies with distance in natural water.

improve the communication quality. From equations (7)–(9), the distance d_1 (d_2) between the transmitting (receiving) electrodes should be as large as possible. Following this principle, the electrodes are arranged at four corners of the shell, as shown in figures 7(a) and (b). To facilitate data analysis, we choose LH and LT as the transmitting electrodes, and RH and RT as the receiving electrodes. Thus, the orientation of transmitting/receiving electrodes is the same as the robot orientation, pointing from the tail electrode to the head electrode.

As shown in figures 7(c) and (d), the communication system occupies a small space and therefore is easy to be integrated into small underwater robots. Since the system is tightly integrated with robot, it will be faced with complex electromagnetic circumstances. Thus, the circuit board is attached onto the upper shell of the robot and encapsulated by copper foil to keep from potential electromagnetic interference.

5. Results and discussion

To demonstrate the effectiveness of the developed robotic electrocommunication system as well as characterize the properties of the developed robotic electrocommunication system, experiments with

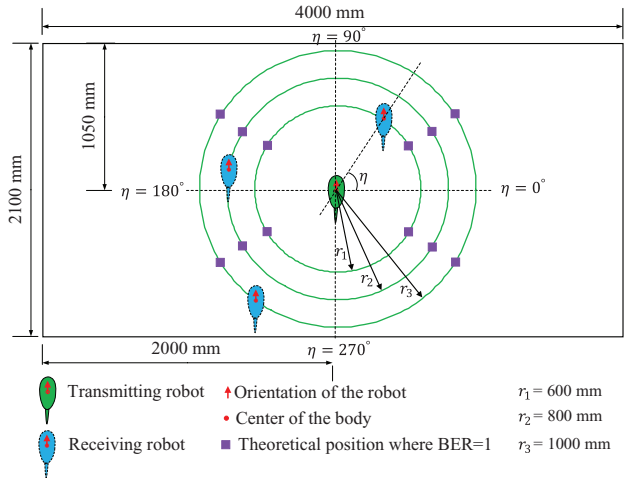

Figure 20. The experimental scene where the receiver changes its position around the transmitter at three fixed distances , r_1, r_2 and r_3, every 1° for $\eta \in (0°, 360°)$. Critical positions that the BER equals to 1 are marked where η are 36°, 144°, 216°, and 324° for r_1, r_2 and r_3.

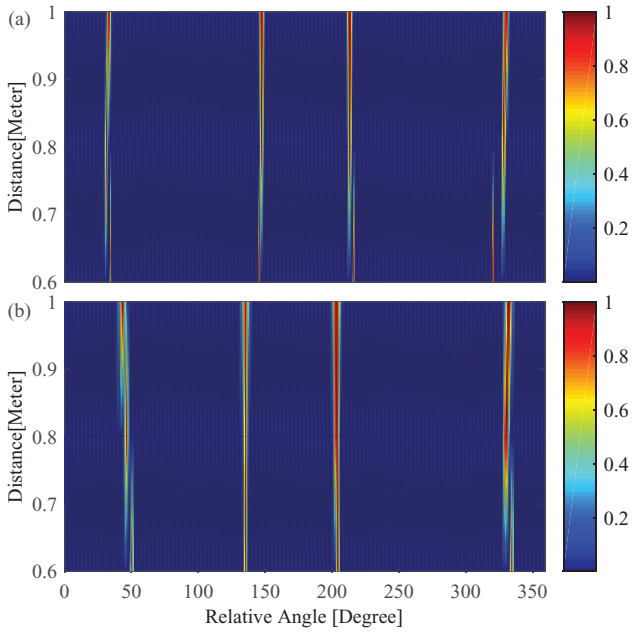

Figure 21. Planar distribution of BER around a transmitting robot/fish model when the emitter and receiver is parallel. BER of each position is the average of five BER readings. Variances are typically less than 0.1% outside the critical areas and typically less than 10% within the critical areas. (a) BER distribution for the fish model. (b) BER distribution for the robot.

the robotic communication system were carried out systematacially in conditions of still water, flowing water, water with obstacle and natural water.

5.1. Experimental description

Four types of experiments were carried out: (1) communication when relative angle between emitter and receiver varies, (2) communication when distance between emitter and receiver varies, (3) communication when receiver changes its position around emitter and (4) robot motion synchronization through electrocommunication. The first three experiments were conducted to characterize the properties of electrocommunication, while the fourth experiment was performed to illustrate potential applications of electrocommunication for a group of underwater robots. Moreover, the first and second types of experiments were conducted in the aforementioned four water conditions, while the third and fourth types of experiments were carried out in still water.

Experiments in still water, flowing water and water with obstacles were conducted in a 4000 mm by 2100 mm polyvinyl chloride (PVC) swimming tank filled with tap water to a depth of approximately 800 mm, as illustrated in figure 8(a). Experiments in natural water were carried out in the Weiming Lake of Peking University, as shown in figure 8(b). The conductivity of tap water is 4.5×10^{-2} S m^{-1}. The water conductivity of Weiming Lake is 7.36×10^{-2} S m^{-1}. The speed of electrocommunication is set at 1200 bps (bits per second) in experiments. As mentioned previously, the consumption of the transmission power is set as $P_t = 0.81$ W.

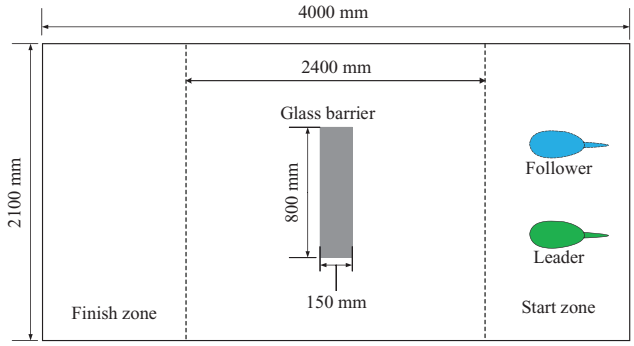

Figure 22. Schematic diagram of robot motion tracking experiment.

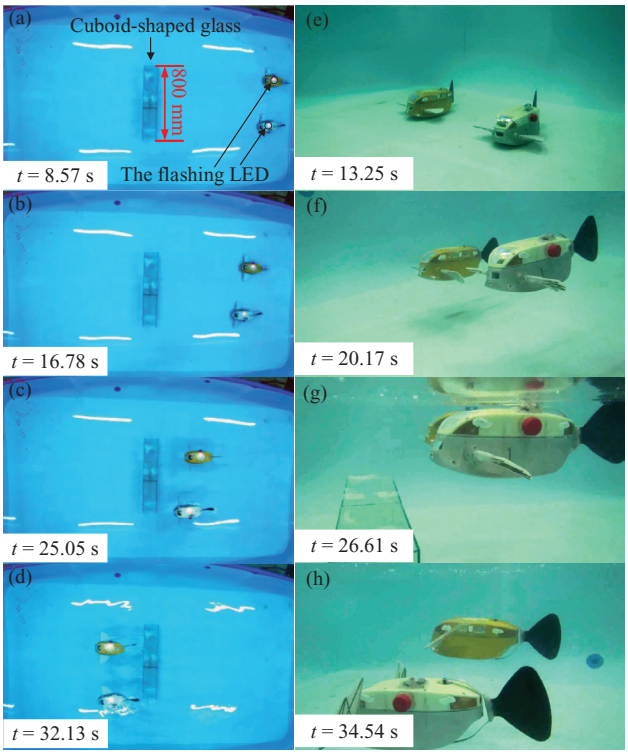

Figure 23. Scenario of motion tracking experiment between the leader and follower using electrocommunication. (a)–(d) respectively show the moments where the leader is sending the command of forward, upward, forward and downward swimming to the follower. At these moments, LEDs on the leader and the follower are flashing. (e)–(h) illustrate the leader and follower synchronously swim forwards at the bottom, upwards, forwards at the surface and downwards, respectively.

In the flowing water experiment, the water was circulated by a centrifugal water pump outside. The pump power is 750 W with maximum flow rate 4.2 $m^3\ h^{-1}$. The flow is turbulent and has a maximum speed of 2.24 m s^{-1}. In the experiment with obstacle, three different sizes 500 mm × 500 mm × 5 mm, 1000 mm × 1000 mm × 5 mm and 1600 mm × 1000 mm × 5 mm) and two different materials (insulator and conductor) of obstacles are explored, as shown in figure 9. The insulated obstacle is made of PVC while the conductive obstacle is made of copper. The obstacle stands centrally and vertically in the water and is perpendicular to the line of two robots, as shown in figure 10. Note that the largest obstacles (shown in figure 10) almost block the whole tank completely.

We use two kinds of physical systems, a pair of fish model and a pair of robotic fish, as shown in figures 11(a) and (b). The fish model is a piece of tempered glass with four identical electrodes in its corners. Electrode layout of fish model is identical to that of the robot. Since the fish model has minimal noises from the robot mechanics and electronics, it can be regarded as a perfect physical model of electrocommunication. All the first three experiments are carried out with a pair of fish model as well as with a pair of robotic fish.

Bit error rate (BER) is adopted to evaluate the communication performance of the first three types of experiments. Both the transmitting and receiving fish model/robot were fixed on the bottom of the tank in these experiments. An azimuth table with 1 degree scale interval are employed to measure the relative angle between the transmitting and receiving fish models/robots, as illustrated in figure 11(a). The position of fish model/robot is defined as the center of the body. For

each trial, the transmitting robot sends 1000 byte data through electrocommunication and the receiving robot accepts and stores the data in a text file. Experimental data were analyzed offline.

5.2. BER distribution when relative angle varies

From the previously mentioned model, the potential difference of receiver changes with its orientation for one position, probably bringing about different performance. We characterize the BER distribution when the relative angle between the fish models/robots varies in still water, flowing water, water with obstacle and natural water. As depicted in figure 12, the transmitting and receiving robots were separated by the distances of 1 m and 2 m in the experiments. Positions of two robots are symmetrical with respect to the midpoint of long and short axes. The relative angle between the fish models/robots is defined as ψ_r, taking the form

$$\psi_r = \psi_2 - \psi_1 \tag{12}$$

where ψ_1 and ψ_2 are orientations of the transmitting robot and the receiving robot, respectively. In the experiment, the transmitting robot was fixed while the receiving robot orientation was changed every 1 degrees from 0° to 360°. Electrocommunication was performed 5 times for each orientation. The ave $(\cdot)$ and var $(\cdot)$ functions were obtained by taking average and variance of 5 times BER data.

5.2.1. *Performance in still water.*

BER distribution for still water is illustrated in figure 13. The receiver's BER remains zero in the vast majority of the orientations for both the fish model and the robot, indicating that electrocommunication does not require precise alignment in practice. Both the fish model and robot have two high BER zones near $\phi_r = 90°$ and $\phi_r = 270°$, which well coincides with model predictions of electrocommunication. More specifically, figure 2 illustrates that the receiver will locate on the equipotential line of emitter's electric field when $\phi_r = 90°$ and $\phi_r = 270°$. In this case, the voltage sensed by the receiver will be zero and BER will be 100% theoretically. In addition, high BER zones at a distance of 2 m are larger than those of 1 m for both the fish model and the robot, also verifying the model that electric field becomes weaker as the distance from the emitter gets larger. A close inspection reveals that fish model's high BER zones are narrower and show better conformity with theoretical angles 90° and 270° compared with the robot's BER distribution. This is due to that electrocommunication between robots is affected by the robot mechanics, motors, sensors and other circuits. These noises from the robot distort the electric field distribution of the emitter. Moreover, these noises weaken the signal detection capacity of receiver, which results in a broader high BER zones.

5.2.2. *Performance in flowing water and water with obstacle.*

Figure 14 shows the experimental results in conditions of flowing water and water with obstacle. First, the two high BER areas in flowing water have little change compared with the results in still water and the high BER angles also close to theoretical values, 90° and 270°, which means that electrocommunication is not affected by water movements. The reason can be easily analysed as follows. The speed of electric field propagation can be calculated

$$\nu = \lambda f = 2\pi f \sqrt{\frac{2}{\omega\mu\sigma}} \tag{13}$$

For our system where $\omega = 2\pi f$, $f = 40$ kHz, $\sigma = 4.5 \times 10^{-2}$ S m^{-1}, $\mu = 1.257 \times 10^{-6}$ H m^{-1}, the propagation speed $\nu = 2.98 \times 10^6$ m s^{-1} and it is about six orders of magnitude larger than the flow speed. Therefore, Doppler effect caused by the water movement can be neglected in electrocommunication. Moreover, we can further deduce that electrocommunication will not be affected by the movements of natural waters whose speeds are typically below the order of 100 m s^{-1}. By contrast, because of the low speed of acoustic propagation in water, of the order of 1500 m s^{-1}, Doppler effect is significant for acoustic communication.

Next, we analysed the communication performance when an obstacle blocked the receiver and transmitter. High BER angles also close to the theoretical values, 90° and 270°, when different obstacles are inserted between the robots/fish models, indicating that electric field distribution is not broken essentially. Similar to the experimental results in still water, the performance of fish model is better than that of the robot when an obstacle is inserted. On the whole, electrocommunication still works well for the majority of explored obstacles in the experiments. By contrast, both optical and acoustic systems are unable to penetrate behind an object and suffer from shadow zones. This superiority makes electrocommunication very practicable to some poor water environments, such as rocky waters and limited sheltered waters. More accurately, large and conductive obstacles have great effects on electrocommunication. To be specific, small obstacle affects the communication scarcely whatever the obstacle is an insulator or conductor. Middle conductive obstacle has small effect while middle insulated obstacle has little effect on the communication. Large conductive obstacle takes great impact while large insulated obstacle has small impact on electrocommunication.

5.2.3. *Performance in natural water.*

Figure 14 shows the BER distribution in which the experiments were conducted in a lake of Peking University. As shown in figure 15, the high BER angles in natural water also approach to the theoretical angles, 90° and 270°. Similarly, electrocommunication quality also

decreases with the distance, and electrocommunication of fish model outperforms that of the robot. However, the ranges of high BER angles for natural water are larger than that of still water. This is probably due to the fact that the electric field is reflected in small tanks. Therefore, the strength of electric field will superpose and become stronger [35] in small tanks. Nevertheless, the electric field in the lake spreads to be as far ahead as possible and not be reflected.

5.3. BER distribution when distance changes

As shown in figure 16, the transmitting robot was fixed at one position near the tank edge. The receiving robot was laterally parallel to the transmitting robot to receive data. As a result, the potential difference of receiver satisfies equation (9) and decreases with distance. The distance r changes from 40 cm to 340 cm every 10 cm. Electrocommunication was performed 5 times for each position. The largest communication distance of current system can be identified.

5.3.1. *Performance in still water.*

Figure 17 presents how the BER changes with the distance of emitter and receiver. It is clear that the fish model has better communication performance than that of the robot. A critical distance d_{cr} is defined as the distance where the BER is equal to 20% in this study. d_{cr} of fish model is more than 4 m but is not obtained because of the size constraint of the tank, while d_{cr} of the robot is about 2.75 m. Similarly, smaller d_{cr} for the robot is mainly due to the large signal noises from the robot mechanics and electronics.

5.3.2. *Performance in flowing water and water with obstacle.*

BER distribution with distance in flowing water and water with obstacle were shown in figure 18. We also use d_{cr} as criteria to evaluate the communication performance. Similar to the results of relative angle experiments, electrocommunication is not affected by the water movements and it works well for most of the explored obstacles. Moreover, electrocommunication of fish model performs better than that of the robot. First, d_{cr} equals about 2.75 m in flowing water and it is identical to the critical distance in still water. Second, d_{cr} is affected by the obstacles in similar ways with relative angle experiments. Specifically, small obstacle affects d_{cr} scarcely no matter the obstacle is an insulator or conductor. Middle conductive obstacle reduces d_{cr} to 2.25 m while middle insulated obstacle still has little impact on d_{cr}. Large conductive obstacle makes the robot communication unattainable while deceases d_{cr} of fish model to 1.80 m. Finally, large insulated obstacle reduces d_{cr} of robot to 2.55 m while impacting barely on fish model communication. Note that middle and large conductive obstacles also greatly affect the communication if the distance between the emitter and receiver is too close.

5.3.3. *Performance in natural water.*

As illustrated in figure 19, in natural water, the critical communication distance of fish model is 340 cm and the critical distance of the robot is 225 cm. The fish model can still communicate at a greater distance than that of the robot. By contrast with the results in the tank, the critical distance in natural water decreases. As a whole, the communication performance declines somewhat in natural water in comparison to the performance in a small tank. This is also caused by the electric field reflection effect [35].

5.4. Planar BER distribution around transmitting robot

If a receiver knows the BER distribution with respect to the position of a transmitter, it can actively adjust its position to acquire a better communication performance. For simplicity, we characterize the planar BER distribution with respect to the transmitter when the transmitter and receiver are in the same direction. The corresponding experiments were carried out as follows. As depicted in figure 20, the transmitter was fixed underwater at the center of the tank, while the receiver was placed at different positions around a circle whose center was the center of the transmitter and whose radius was the distance r between centers of two fish models/robots. The bearing angle η was defined to describe the planar position of the receiver with respect to the transmitter. In the experiment, the receiver position was changed every 1 degree from 0° to 360° for radius of 0.6 m, 0.8 m and 1 m. Electrocommunication was conducted 5 times for each position of receiver. Theoretical positions where BER was equal to one were defined as critical positions. These critical positions were calculated according to the dipole model in section 2, and marked in figure 20. The corresponding bearing angles η are around 36°, 144°, 216° and 324° for the three distances.

Receiver's planar BER distributions around an transmitter when the transmitter and receiver are parallel in electrocommunication are illustrated in figure 21. It is obvious that BER is zero for most planar positions of the receiving robot/fish model. Combining the BER distribution in the angle change experiment above, we conclude that the bio-inspired electrocommunication is almost omnidirectional in terms of both position and angle. Similar to the distribution of four theoretical critical positions in figure 20, there are four conspicuous areas with high BER for both the fish model and the robot in the experiments. More specifically, four central positions of high BER are 33°, 147°, 214° and 326° for fish model, and 46°, 135°, 204° and 332° for the robot. Central positions of high BER areas of fish model are nearly consistent with the theoretical critical positions while central positions of high BER areas of the robot shift about 10° compared with the theoretical results. This is also caused by the small distortion of electric field when the communication system is working with the robot. Moveover, high BER areas of the robot and

the fish model become broader as the distance increases from 0.6 m to 1 m. This is due to the fact that the electric field strength and the potential difference between the receiving electrodes decrease rapidly as the distance between the receiver and transmitter become larger. We therefore speculate that the high BER areas will become broader as the distance increases further.

5.5. Motion synchronization using Electrocommunication

This section demonstrates the potentials of electrocommunication in underwater task execution within the control scope. In particular, we illustrate that a leader robotic fish guides a follower robotic fish to cross a cuboid-shaped glass barrier autonomously in the three-dimensional space.

The sketch map of the experiment is shown in figure 22. At the beginning, the two robots were placed at the bottom of the tank parallel laterally with each other in the start zone. Then, the leader conducted a serious of swimming behaviors autonomously to pass over the barrier and reached the finish zone. Whenever the leader started a new behavior, it sent the behavior to the follower by electrocommunication simultaneously. Through communication, the follower can always track the leader and pass over the barrier. Communication protocol was the same as the one described in our previous experiments [40]. The trial succeeded if the follower tracked all the swimming behaviors of the leader correctly and passed over the barrier.

Experimental results show that the follower is able to track the leader and finish the task through electrocommunication. We conducted 100 trials and 71% were successful. Note that each command is sent only once for each behavior and the success rate can be easily improved by sending repeated command. A more formal solution to improve the success rate as well as lower the delivery cost is to design robust communication protocol in terms of communication distance and relative angle between the robots. Several experimental snapshots are illustrated in figure 23. LEDs onboard the leader and follower flicker timely to indicate the electrocommunication. From figures 23(a)–(d), LEDs on the robots flashed almost simultaneously, suggesting that there was little time delay in electrocommunication. We have calculated the propagation velocity of our electrocommunication system above via equation (13) where $\nu = 2.98 \times 10^6\,\mathrm{m\,s^{-1}}$. This propagation velocity is much higher than that of the acoustic communication (where $\nu = 1.50 \times 10^3\,\mathrm{m\,s^{-1}}$). That is, the propagation velocity of the electrocommunication is almost 2000 times faster than that of the acoustic communication. As a result, the time delay of electrocommunication will be typically much shorter than that of acoustic communication. Therefore, electrocommunication would be more preferable to acoustic method for multi-robot control tasks with low-delay requirement.

5.6. Discussion

Multi-robot control has been drawing more and more attentions in recent years, and communication plays an essential role in the control of multiple robots. Due to the particularity of water medium (for instance, radio-frequency signals attenuate drastically in water), communication of underwater robots is tricky and has not been currently solved satisfactorily, especially for those small robots that always operate in cluttered, limited underwater environment. In this paper, inspired by electrocommunication of weakly electric fish in nature, we design an artificial electrocommunication system and then integrate this bio-inspired communication system into our bio-inspired fish robots to demonstrate the feasibility for underwater cooperative control. By using this bio-inspired communication system, we show that a swimming fish robot is able to communicate steadily with another robot within a range of about three meters.

Compared with traditional acoustic and optical methods, the developed electrocommunication has several advantages. First, due to its nature properties, electrocommunication can barely be disturbed by most of the noises in water environments, such as water movements, temperature and density variation in the water. In particular, flowing water experiments in this paper have partly validated that electrocommunication is free from water movements. In comparison, acoustic communication can be influenced by many noise factors in the water environments [21], for instance, shipping activity and movement of water including tides, current, storms, wind, and rain. Second, theoretical analysis and experimental results have demonstrated that electrocommunication can be regarded as an omnidirectional communication, while optical communication has directionality and require accurate calibration [22]. As a result, electrocommunication will be more suitable than optical method for mobile underwater robots. Third, obstacle experiments in this paper show that electrocommunication is almost not affected by most types of obstacles in the water. By contrast, it is generally accepted that acoustic method will face great challenges of multi-path effects when obstacles exist between the transceiver. At the same time, the optical method is susceptive to water turbidity and therefore it is easily blocked by obstacles in water. Moreover, the working principle of electrocommunication is different with the RF communication described in [24, 25]. In RF communication, the signal is radiated in the form of displacement current, while in electrocommunication, the signal is delivered in the form of conductive current. The authors mentioned that RF communication was not very stable underwater [25]: 'many packets failed a checksum test or were lost entirely. The success rate of packet delivery is difficult to quantify as it varied with the relative positions and orientations of the vehicles'. While experimental results in this paper show that electrocommunication is very stable for information deliver and the bit error rate is zero for most of the relative positions and orientations. To sum

up, electrocommunication is a very promising approach for complex water areas such as turbid, rocky and coastal, and suitable to small underwater robots that have stringent power and size constraints.

Regarding the limitation of electrocommunication, we would like to emphasize two points. First, the current effective distance of electrocommunication is typically 3 m, which may restrict the robot motion space in a group, thereby reducing the group flexibility. The effective range can be enlarged by increasing the emitting power and/or improving the signal to noise ratio through specialized filtering circuits. Second, due to the nature of electric fields, electrocommunication will fail in several situations where the receiver is almost parallel to its nearby isopotential line of the electric field generated by the emitter. This can be solved initially by sending duplicate data. For instance, useful information can be sent twice during electrocommunication. More formally, a request/reply mechanism should be added to the communication protocol to ensure the success of communication.

Further, jamming and overlapping may occur when two or more robots are generating electric signals simultaneously in a group. To deal with the jamming problem, we suggest a collision detection mechanism that can be introduced into the communication, such as the carrier sense multiple access/collision detected (CSMA/CD) protocol used in Ethernet communication. In short, the state of the communication channel can be always checked before any data transmission. If the channel is busy, the individual should wait until the channel is idle. On the other hand, biological experiments [45, 46] revealed that weakly electric fish use specific strategies to organize their collective electric activity. In particular, they order their electric activity of each member of a group in a fixed sequence of individual pulses separated by 'silent periods' to solve the jamming problem. This method looks simple and stable for a group of individuals. These two methods could be further studied in the future to make electrocommunication more practical for multi-robot communication.

6. Conclusion and future work

In this paper, we have designed a bio-inspired electrocommunication system for small underwater robots and integrated the system into our robotic fish to demonstrate its effectiveness in robotics as well as characterize its communication performance. Using this communication approach, the small robotic fish can communicate with each other efficiently within a range of about 3 m at a speed of around 1 k baud in an almost omnidirectional vision. Experiments in conditions of still water, flowing water, water with obstacles and natural water have shown that electrocommunication is not affected by water movements and most types of obstacles, and it still works well in nature water. We also demonstrate that a leader robot could guide a follower robot to pass over a barrier autonomously in a three-dimensional water space by use of electrocommunication. Electrocommunication is a very inexpensive approach for underwater robots because the sensors are simply exposed conductors, and the signal processing circuits are uncomplicated. Strengths like the small size, low cost, low power, approximate omni-directivity, and high adaptability to water conditions, probably bring electrocommunication to be a useful complement to the usual suite of sensors provisioned on standard underwater robots in the near future.

For the purpose of studying multi-robot control with our autonomous robotic fish, we will continue focusing on the enhancement of the communication distance and the design of a robust communication protocol in our future work. And this electrocommunication system will be critical for the formation control of future underwater team robots.

Acknowledgments

This work was supported in part by grants from the National Natural Science Foundation of China (NSFC, No. 51575005, 61503008, 61633002, 91648120) and the China Postdoctoral Science Foundation (No. 2015M570013, 2016T90016). We would like to thank DENG Hanbo and ZHOU Yang for their contributions in carrying out the experiments with the robot, thank WANG Zijian and WANG Zerui for their contributions in robot design, thank LI Liang and WANG Chen for their contributions for valuable discussions, and finally thank CAO Fayang for his contributions in circuit implementation. In addition, the authors would like to thank the anonymous reviewers for their valuable comments and suggestions on improving the manuscript.

References

[1] Ijspeert A J, Crespi A, Ryczko D and Cabelguen J M 2007 From swimming to walking with a salamander robot driven by a spinal cord model *Science* **315** 1416–20
[2] Ijspeert A J 2014 Biorobotics: using robots to emulate and investigate agile locomotion *Science* **346** 196–203
[3] Liu J and Hu H 2010 Biological inspiration: from carangiform fish to multi-joint robotic fish *J. Bionic Eng.* **7** 35–48
[4] Hu Y, Zhao W and Wang L 2009 Vision-based target tracking and collision avoidance for two autonomous robotic fish *IEEE Trans. Ind. Electron.* **56** 1401–10
[5] Zhou C and Low K H 2012 Design and locomotion control of a biomimetic underwater vehicle with fin propulsion *IEEE/ASME Trans. Mechatronics* **17** 25–35
[6] Feitian Z, Thon J, Thon C and Xiaobo T 2014 Miniature underwater glider: design and experimental results *IEEE/ASME Trans. Mechatronics* **19** 394–9
[7] Crespi A, Lachat D, Pasquier A and Ijspeert A J 2008 Controlling swimming and crawling in a fish robot using a central pattern generator *Auton. Robots* **25** 3–13
[8] Nor N M and Ma S 2014 Smooth transition for CPG-based body shape control of a snake-like robot *Bioinspiration Biomimetics* **9** 016003
[9] Yu J, Wang M, Tan M and Zhang J 2011 Three-dimensional swimming *IEEE Trans. Robot. Autom.* **18** 47–58
[10] Seo K, Chung S J and Slotine J J E 2010 CPG-based control of a turtle-like underwater vehicle *Auton. Robots* **28** 247–69

[11] Morgansen K A, Triplett B I and Klein D J 2007 Geometric methods for modeling and control of free-swimming fin-actuated underwater vehicles *IEEE Trans. Robot. Autom.* **23** 1184–99
[12] Yu J, Su Z, Wang M, Tan M and Zhang J 2012 Control of yaw and pitch maneuvers of a multilink dolphin robot *IEEE Trans. Robot.* **28** 318–329
[13] Marchese A D, Onal C D and Rus D 2014 Autonomous soft robotic fish capable of escape maneuvers using fluidic elastomer actuators *Soft Robot.* **1** 75–87
[14] Wen L, Wang T, Wu G and Liang J 2013 Quantitative thrust efficiency of a self-propulsive robotic fish: experimental method and hydrodynamic investigation *IEEE/ASME Trans. Mechatronics* **18** 1027–38
[15] Salumäe T and Kruusmaa M 2013 Flow-relative control of an underwater robot *Proc. R. Soc.* A **469** 2153
[16] Zhang D, Wang L, Yu J and Tan M 2007 Coordinated transport by multiple biomimetic robotic fish in underwater environment *IEEE Trans. Control Syst. Technol.* **15** 658–71
[17] Yang E and Gu D 2007 Nonlinear formation-keeping and mooring control of multiple autonomous underwater vehicles *IEEE/ASME Trans. Mechatronics* **12** 164–78
[18] Jia Y and Wang L 2015 Leader-follower flocking of multiple robotic fish *IEEE/ASME Trans. Mechatronics* **30** 1–12
[19] Butail S, Bartolini T and Porfiri M 2013 Collective response of zebrafish shoals to a free-swimming robotic fish *PLoS One* **8** e76123
[20] Kilfoyle D B, Kilfoyle D B and Baggeroer A B 2000 The state of the art in underwater acoustic telemetry *IEEE J. Ocean. Eng.* **25** 4–27
[21] Akyildiz I F, Pompili D and Melodia T 2005 Underwater acoustic sensor networks: research challenges *Ad hoc Netw.* **3** 257–79
[22] Hanson F and Radic S 2008 High bandwidth underwater optical communication *Appl. Opt.* **47** 277–83
[23] Arnon S 2010 Underwater optical wireless communication network *Opt. Eng.* **49** 015001
[24] Bettale P K 2008 Design of a reliable embedded radio transceiver module with applications to autonomous underwater vehicle systems *Master's Thesis* University of Washington
[25] Klein D J, Gupta V and Morgansen K A 2011 Coordinated control of robotic fish using an underwater wireless network (New York: Springer) pp 323–39
[26] Lissmann H W and Machin K E 1958 The mechanism of object location in gymnarchus niloticus and similar fish *J. Exp. Biol.* **35** 451–86
[27] Moller P 1995 *Electric Fishes Behavior* (*Fish and Fisheries Series*) (London: Chapman and Hall)
[28] Kramer B 1996 Electroreception and communication in fishes *Progress in Zoology* vol 42 (Stuttgart: Gustav Fischer)
[29] Bai Y, Snyder J B, Peshkin M and MacIver M A 2015 Finding and identifying simple objects underwater with active electrosense *Int. J. Robot. Autom. Res.* **34** 1255–77
[30] Chevallereau C, Benachenhou M-R, Lebastard V and Boyer F 2014 Electric sensor-based control of underwater robot groups *IEEE Trans. Robot.* **30** 604–18
[31] Momma H and Tsuchiya T 1976 Underwater communication by electric current *Oceans* 631–6
[32] Tucker M J 1972 Conduction signalling in the sea *Radio Electron. Eng.* **42** 453
[33] Al-Shamma'a A I, Shaw A and Saman S 2004 Propagation of electromagnetic waves at MHz frequencies through seawater *IEEE Trans. Antennas Propag.* **52** 2843–9
[34] Grimaccia F, Gandelli A, Johnstone R W, Chiffings T and Zich R E 2005 Smart integrated sensor networks for the marine environment *Proc. SPIE* **6035** 603513
[35] Joe J and Toh S H 2007 Digital underwater communication using electric current method *Oceans* 1–4
[36] Kim C W, Lee E and Syed N A A 2010 Channel characterization for underwater electric conduction communications systems *Oceans* 1–6
[37] Friedman J K 2009 Electrostatic transconduction for underwater communication and imaging *PhD Thesis* Citeseer
[38] Esemann T, Ardelt G and Hellbrück H 2014 Underwater electric field communication *Proc. Int. Conf. Underwater Networks & Systems* (ACM) p 9
[39] Zoksimovski A, Sexton D, Stojanovic M and Rappaport C 2015 Underwater electromagnetic communications using conduction c channel characterization *Ad hoc Netw.* **34** 42–51
[40] Wang W, Zhao J, Xiong W, Cao F, Xie G 2015 Underwater electric current communication of robotic fish: design and experimental results *2015 IEEE Int. Conf. Robotics and Automation* pp 1166–71
[41] Carr C E, Maler L and Sas E 1982 Peripheral organization and central projections of the electrosensory nerves in gymnotiform fish *J. Comparative Neurol.* **211** 139–53
[42] Bullock T H, Hopkins C D, Popper A N and Fay R R 2005 *Electroreception* (NewYork: Springer)
[43] Wang W, Guo J, Wang Z and Xie G 2013 Neural controller for swimming modes and gait transition on an ostraciiform fish robot *IEEE/ASME Int. Conf. Advanced Intelligent Mechatronics* pp 1564–9
[44] Wang W and Xie G 2014 CPG-based locomotion controller design for a boxfish-like robot *Int. J. Adv. Robot. Syst.* **11** 87
[45] Bullock T H, Hamstra R H Jr and Scheich H 1972 The jamming avoidance response of high frequency electric fish, part (i) and part (ii) *J. Comparative Physiol.* **77** 1–48
[46] Stamper S A, Madhav M S, Cowan N J and Fortune E S 2012 Beyond the jamming avoidance response: weakly electric fish respond to the envelope of social electrosensory signals *J. Exp. Biol.* **215** 4196–207